

Joint Channel-Diversity Coding for the Three-Way Free-Space Optical Systems through Atmospheric-Turbulence Channels

Chadi Abou-Rjeily

Department of Electrical and Computer Engineering
Lebanese American University, Byblos, Lebanon
chadi.abourjeily@lau.edu.lb

ABSTRACT

In this paper, we study the communications over the free-space optical (FSO) links in the presence of atmospheric turbulence that induces strong fading on the FSO channel. We consider the three-way systems where a wireless transceiver (or relay) that is present in the neighborhood of the source and destination shares its resources for assisting the source in delivering its message to the destination. In particular, we derive the error performance of the three-way FSO systems that are implemented with a convenient combination of channel and diversity coding. This joint channel-diversity coding that is associated with adapted decoding at the relay and the destination results in a better immunity against noise and fading and results in high performance levels over a very wide range of the signal-to-noise ratio. Another appealing feature of the considered system resides in the fact that the error protection is not associated with any reduction in the data rate.

KEYWORDS

Free-Space Optics, turbulence atmospheric channels, FSO, cooperation, channel coding, diversity coding, error correction, binary symmetric channel (BSC), binary erasure channel (BEC).

1 INTRODUCTION

Free-Space Optical (FSO) communications constitute an appealing solution for wireless access networks

where the large bandwidth of the optical signals makes it possible to achieve very high data-rates over the wireless links. Moreover, FSO systems are characterized by a remarkable simplicity in terms of the architecture of the deployed FSO transceivers since intensity modulation (IM) is implemented at the transmitter side while simple non-coherent direct detection (DD) is implemented at the receiver side [1]-[3]. Moreover, FSO links constitute a cost-effective solution to the “last mile” problem where optical transceivers deployed at the roofs of buildings avoid digging for the installation of optical fibers.

On the other hand, FSO links suffer from several impairments that might severely degrade the link quality. These impairments include fading (or scintillation) that results from the variations of the index of refraction due to inhomogeneities in temperature and pressure changes [1]. In this case, the performance of FSO links drops and the connection might even be lost because of atmospheric turbulence that constitutes a critical parameter in determining the performance of these long-distance FSO links. In order to mitigate these impairments and leverage the performance of FSO systems, several techniques were applied in the literature. These include error control coding that is deployed in conjunction with interleaving [4], multiple-symbol

detection [5] and spatial diversity [6]-[10].

Among all the previous techniques, the spatial diversity techniques are appealing because of their capability in achieving high multiplexing and diversity gains [6]. Spatial diversity can be realized in a localized manner by deploying multiple lasers at the transmitter side and multiple photo-detectors at the receiver side [6]. These FSO localized diversity techniques are inspired from the well known Multiple-Input-Multiple-Output techniques that were studied extensively in the context of radio frequency (RF) wireless communications. In this context, localized FSO diversity techniques include aperture-averaging receiver diversity [7], spatial repetition codes [8], unipolar versions of the orthogonal space-time codes [9] and transmit laser selection [10]. However, these techniques suffer mainly from the channel correlation that is particularly pronounced in FSO systems. In fact, for RF systems, the wide beamwidth of the antennas and the rich scattering environment that is often present between the transmitter and the receiver both ensure that the signal reaches the receiver via a large number of independent paths. Consequently, the assumption of spatially uncorrelated channels is often valid for these systems. On the other hand, for FSO links, the laser's beamwidth is very narrow and these links are much more directive thus rendering the assumption of uncorrelated channels practically not valid for these systems. For example, the presence of a small cloud might induce large fades on all source-detector sub-channels simultaneously [8]. Consequently, the high performance gains promised by MIMO-FSO systems might not be

achieved in practice and "*alternative means of operation in such environments must be considered*" [8].

Another way for realizing spatial diversity is based on distributed techniques where neighboring nodes in a wireless network cooperate with each other to form a "virtual" antenna array and profit from the underlying spatial diversity in a distributed manner. Recently, such techniques started attracting significant attention in the context of FSO communications where several Amplify-and-Forward (AF) strategies [11] as well as Decode-and-Forward (DF) strategies [12]-[15] were proposed and analyzed. However, despite this increasing interest in cooperation in FSO systems, previous contributions were either based exclusively on diversity coding without any reference to channel coding [12]-[14] or were based on a layered implementation of diversity and channel coding where the channel code was implemented independently from the underlying diversity code [15]. In this last case, the considered channel encoding/decoding schemes do not take the structure of the implemented cooperation strategy into consideration.

In this paper, we consider the problem of joint channel-diversity coding where the cooperation strategy and error-correction are implemented in conjunction. In other words, the structure of the cooperation strategy (diversity code) depends on the channel encoding scheme and vice versa. In this context, the main contribution of this paper consists of proposing two novel cooperation strategies for the three-way FSO systems where direct links are assumed to be available between the source-destination, source-relay and relay-destination. In both

schemes, the information symbols are transmitted over the direct source-destination link while the parity symbols are transmitted over the indirect source-relay-destination link. Consequently, unlike non-cooperative systems where channel coding results in reduced data-rates, the considered systems are not associated with any reduction in the data rate. On the other hand, the difference between these strategies is highlighted in what follows. In the first strategy all the symbols that are received at the relay are decoded and retransmitted to the destination; in this case, hard decisions are made at the relay and destination. On the other hand, the second strategy applies some form of selectivity on the symbols to be forwarded to the relay. In this case, the relay backs off if the quality of the signal received by the relay does not ensure a correct detection at the destination. Moreover, in this second strategy, the relay and destination make decisions only on some symbols while erasures are declared on the remaining symbols. In other words, the first scheme resembles a parallel three-way binary symmetric channel (BSC) while the second scheme corresponds to a parallel three-way binary erasure channel (BEC). Finally, we derive exact expressions of the bit-error-rates (BER) of both joint diversity-channel protocols and we prove the superiority of the second scheme that results in a better rejection of shot noise and in a better immunity against fading.

2 SYSTEM MODEL

Consider the three-way cooperative FSO systems depicted in Fig. 1. The links between the source (S), relay (R) and destination (D) are established via FSO-based wireless units each consisting of

an optical transceiver with a transmitter and a receiver to provide full-duplex capability. Given the high directivity and non-broadcast nature of FSO transmissions, one separate transceiver is entirely dedicated for the communication between each couple of nodes. In this context, the three links between S-D, S-R and R-D are parallel and do not interfere with each other.

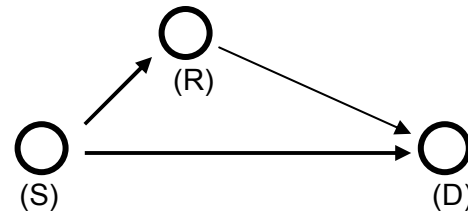


Figure 1. The three-way cooperative FSO system.

Denote by a_0 , a_1 and a_2 the random path gains between S-D, S-R and R-D, respectively. In this work, we adopt the Rayleigh turbulence-induced fading channel model [6] where the probability density function (pdf) of the path gain ($a > 0$) is given by:

$$f_A(a) = 2a \exp(-a^2) \quad (1)$$

We consider binary pulse position modulation (PPM) with IM/DD. In this case, each receiver corresponds to a photoelectrons counter that counts the number of electrons received in each PPM slot. We also consider the case of shot-noise limited FSO systems that do not suffer from background radiation and dark currents. In this case, the only source of noise in these systems is the shot noise that results from the light signal itself. Denote by λ_s the average number of photoelectrons per slot resulting from the incident light signal. This parameter is given by [6]:

$$\lambda_s = \eta \frac{P_r T_s}{2hf} \quad (2)$$

where:

- η is the detector's quantum efficiency assumed to be equal to 1 in what follows.
- $h = 6.6 \cdot 10^{-34}$ is Planck's constant.
- T_s is the symbol duration.
- f is the optical center frequency corresponding to a wavelength of 1550 nm.
- P_r stands for the optical signal power that is incident on the receiver.

We define E_s as the received optical energy per PPM slot corresponding to the direct link S-D which can be written as:

$$E_s = \frac{P_r T_s}{2} \quad (3)$$

We consider the case where a (N,K) block channel code is applied where K information bits are encoded into codewords having a length N. As a first step of the cooperation strategies that we propose in this paper, the K information bits are mapped into K binary PPM symbols and transmitted along the direct link S-D. At a second time, the N-K redundant parity bits are mapped into N-K PPM symbols and transmitted to the relay R along the link S-R. In what follows, the information symbols will be denoted by s_1, \dots, s_K while the parity symbols will be denoted by c_1, \dots, c_{N-K} . All of these symbols are taken from the set $\{1,2\}$ that represents the PPM constellation. We denote by $X_k = [X_{k,1} \ X_{k,2}]$ the 2-dimensional vector corresponding to the number of photoelectrons detected at the destination in the two PPM slots corresponding to the symbol s_k for $k=1 \dots K$. Since we are considering the case of no background radiation, one component of the vector X_k will be equal to zero (this corresponds to the empty

slot) while the other component (which corresponds to the number of photoelectrons in the transmitted PPM slot) can be modeled as a Poisson random variable (r.v.) whose parameter is given by:

$$E[X_{k,s_k}] = \frac{K}{N} a_0^2 \lambda_s \quad (4)$$

where $E[.]$ stands for the averaging operator. In the last equation, the factor K/N corresponds to a power normalization that will be justified later. In the same way, we denote by $Y_k = [Y_{k,1} \ Y_{k,2}]$ the 2-dimensional vector corresponding to the photoelectron counts observed at the relay in the two PPM slots corresponding to the symbol c_k for $k=1 \dots N-K$. In this case, the number of photoelectrons in the non-empty plot can be modeled as a Poisson r.v. whose parameter is given by:

$$E[Y_{k,c_k}] = \frac{1}{2} \frac{N-K}{N} \beta_1 a_1^2 \lambda_s \quad (5)$$

where β_1 is a gain factor that follows from the fact that S might be closer to R than it is to D. In other words, the energy E_s received at D corresponds to the energy $\beta_1 E_s$ at R. Performing a typical link budget analysis [6] shows that

$$\beta_1 = \left(\frac{d_{SD}}{d_{SR}} \right)^2 \quad \text{where } d_{SD} \text{ and } d_{SR} \text{ stand}$$

for the distances from S to D and from S to R, respectively.

The relay will retransmit the symbols r_1, \dots, r_{N-K} along the link R-D. The way in which these symbols are determined depends on the specific cooperation strategy and will be explained in the following sections. In this case, the decision vector at D corresponding to the link R-D will be denoted by $Z_k = [Z_{k,1} \ Z_{k,2}]$ for $k=1 \dots N-K$. The

component of Z_k corresponding to the nonempty slot is modeled as a Poisson r.v. with parameter:

$$E[Z_{k,r_k}] = \frac{1}{2} \frac{N-K}{N} \beta_2 a_2^2 \lambda_s \quad (6)$$

where $\beta_2 = \left(\frac{d_{SD}}{d_{RD}} \right)^2$ and d_{RD} stands for the distance between R and D.

From equations (4), (5) and (6), normalizing the powers along the links S-D, S-R and R-D by $\frac{K}{N}$, $\frac{K-N}{2N}$ and $\frac{K-N}{2N}$, respectively, ensures that the coded cooperative systems transmit the same amount of power as the uncoded non-cooperative systems. Note that the power transmitted along the indirect link S-R-D is equally distributed among the two hops S-R and R-D.

Note that for non-cooperative systems, the K information bits and $N-K$ parity bits are transmitted serially from the source to the destination resulting in a data-rate reduction by a factor of K/N . On the other hand, for the proposed cooperation strategies, the information and parity bits are simultaneously transmitted in parallel along the direct link S-D and indirect link S-R-D, respectively. This results in the fact that the proposed cooperation strategies transmit at exactly the same data-rate as non-cooperative systems implying that error correction is not achieved at the expense of a data-rate reduction.

3 SCHEME-1: PARALLEL BSC CHANNEL

The cooperation strategies differ from each other by the decoding and

retransmission strategies at the relay and by the decoding at the destination.

3.1 Cooperation Strategy

Consider the vector Y_k received at the relay. Given that one component of Y_k (corresponding to the empty slot) is always equal to zero, then two cases are possible at this relay. (i): One component of Y_k is different from zero. This implies that the PPM symbol was transmitted in this slot since in the absence of background radiation; the only source of this nonzero count is the presence of a light signal in the corresponding slot. In this case, R decides in favor of the nonempty slot and the decision it makes is correct. In other words, $r_k=c_k$ for k belonging to the set $\{1, \dots, N-K\}$. (ii): Both slots are empty where because of shot noise and fading; the light signal does not generate any photoelectrons. In this case, the best that the relay can do is to break the tie randomly and decide in favor of any one of the two slots resulting in an erroneous decision with probability $1/2$.

Concerning the relay, the first cooperation strategy is as follows: if one detected slot in Y_k is different from zero, the relay decides in favor of $r_k=c_k$ and transmits this symbol. On the other hand, when Y_k is equal to the all-zero vector, the relay decides randomly in favor of one slot r_k in $\{1,2\}$ and forwards its decision to the destination. In this case, the three-way FSO system is analogous to a parallel BSC channel where the transmitted symbol is taken from $\{1,2\}$ while the decoded symbol belongs to the same set. The above scheme will be referred to as scheme-1 in what follows. The decoding strategy at the destination will be explained in section 3.3.

3.2 Raw Bit-Error-Rate

Proposition 1: for scheme 1, the conditional BER along the indirect link S-R-D is given by:

$$p_1 = \frac{1}{2} [e^{-k_1} + e^{-k_2} - e^{-(k_1+k_2)}] \quad (7)$$

where the constants k_1 and k_2 are given by:

$$k_i = \frac{1}{2} \frac{N-K}{N} \beta_i a_i^2 \lambda_s ; i = 1, 2 \quad (8)$$

Proof: assume that the symbol $c_k \in \{1, 2\}$ was transmitted along the link S-R while the relay decided in favor of symbol $r_k \in \{1, 2\}$ and transmitted this symbol along the link R-D. In this case, the probability of error can be written as:

$$p_1 = \Pr(Z_{k,r_k} = 0) p_{1,1} + \Pr(Z_{k,r_k} > 0) p_{1,2} \quad (9)$$

where $p_{1,1} = \frac{1}{2}$ since the case $Z_{k,r_k} = 0$ implies that the vector Z_k will be equal to the all-zero vector implying that a random decision will be made at D resulting in an erroneous hit with probability $\frac{1}{2}$. On the other hand, when $Z_{k,r_k} > 0$, D will decide in favor of the symbol r_k . In this case, an error will be made at D if an error was made at R and a correct decision will be made at D if a correct decision was made at R. In other words, $p_{1,2} = p_e^{(R)}$ where $p_e^{(R)}$ stands for the probability of error at the relay. Given that an error is made at the relay with probability $\frac{1}{2}$ when both components of vector Y_k are zero, then:

$$p_e^{(R)} = \frac{1}{2} \Pr(Y_{k,c_k} = 0) = \frac{1}{2} e^{-k_1} \quad (10)$$

following from equations (5) and (8). On the other hand, from equations (6) and (8) $\Pr(Z_{k,r_k} = 0) = 1 - \Pr(Z_{k,r_k} > 0) = e^{-k_2}$. Consequently, equation (9) can be written as:

$$p_1 = e^{-k_2} \frac{1}{2} + (1 - e^{-k_2}) \frac{1}{2} e^{-k_1} \quad (11)$$

which simplifies to equation (7).

3.3 Coded Bit-Error-Rate

After determining the uncoded raw error probability along the indirect link, we next evaluate the BER at the destination. The decoding procedure along the link S-D is the same as that over the link S-R-D. In other words, the restored information symbols along S-D are given by (for $k=1 \dots K$):

$$\hat{s}_k = \begin{cases} \arg[X_k \neq 0]; & X_k \neq [0 \ 0] \\ \text{rand}(1,2); & X_k = [0 \ 0] \end{cases} \quad (12)$$

where the function $\text{rand}(1,2)$ corresponds to randomly selecting one element of the set $\{1, 2\}$. On the other hand, the restored parity symbols along the link S-R-D can be written as (for $k=1 \dots N-K$):

$$\hat{c}_k = \begin{cases} \arg[Z_k \neq 0]; & Z_k \neq [0 \ 0] \\ \text{rand}(1,2); & Z_k = [0 \ 0] \end{cases} \quad (13)$$

In what follows, we denote by p_0 the raw probability of error along the direct link S-D:

$$p_0 = \frac{1}{2} \Pr(X_{k,s_k} = 0) = \frac{1}{2} e^{-k_0} \quad (14)$$

The destination will determine the most probable values of the transmitted symbols $s_1 \dots s_K$ based on the detected vector $S = [\hat{s}_1 \ \dots \ \hat{s}_K \ \hat{c}_1 \ \dots \ \hat{c}_{N-K}]$ having a length N . In this case, the decoding procedure at D will be the same as the conventional decoding rules of linear channel block codes; in other words, maximum-likelihood (ML) decoding or syndrome decoding can be applied. In this case, the channel code is capable of correcting any vector S having t or fewer errors where:

$$t = \left\lfloor \frac{d_{\min} - 1}{2} \right\rfloor \quad (15)$$

where d_{\min} stands for the minimum Hamming distance of the block code.

Denote by t_0 the number of errors among $\hat{s}_1 \dots \hat{s}_K$ along the direct link S-D and by t_1 the number of errors among the symbols $\hat{c}_1 \dots \hat{c}_{N-K}$ received via the indirect link. As long as $t_0 + t_1 \leq t$, the number of errors is within the error correction capabilities of the channel code and no error will be made at the output of the decoder. Consequently, the probability of error at the output of the decoder conditioned on the channel state vector $A = [a_0 \ a_1 \ a_2]$ can be written as:

$$P_{e|A} \leq \sum_{i=t+1}^N \sum_{t_0=1}^{\min(i,K)} \sum_{\substack{t_1=1 \\ t_0+t_1=i}}^{\min(i,N-K)} \binom{K}{t_0} p_0^{t_0} (1-p_0)^{K-t_0} \binom{N-K}{t_1} p_1^{t_1} (1-p_1)^{N-K-t_1} \quad (16)$$

where the error probability along the indirect link (p_1) is given in eq. (7) while the error probability along the direct link (p_0) is given in eq. (14). Equation (16) reflects the distribution of the errors among the direct and indirect links. The

number $\binom{K}{t_0}$ corresponds to the possible number of positions of the t_0 erroneous symbols among $\hat{s}_1 \dots \hat{s}_K$ while $p_0^{t_0}$ stands for the probability of having t_0 binary symbols flipped while $(1-p_0)^{K-t_0}$ stands for the probability of correctly detecting the remaining $K-t_0$ symbols. In the same way, $\binom{N-K}{t_1}$, $p_1^{t_1}$ and $(1-p_1)^{N-K-t_1}$ stand for the number of combinations of the t_1 erroneous symbols among the $N-K$ symbols $\hat{c}_1 \dots$

\hat{c}_{N-K} , the probability of having these t_1 symbols in error and the probability of making correct decisions on the remaining $N-K-t_1$ symbols, respectively. Note that eq. (16) is analogous to the expression of the conditional error probability of (N,K) block codes along single-input-single-output (SISO) links that is given by:

$$P_{e|A} \leq \sum_{i=t+1}^N \binom{N}{i} p^i (1-p)^{N-i} \quad (17)$$

where p stands for the raw probability of error along this SISO link. The only difference between equations (16) and (17) resides in distributing the errors among the direct and indirect links. Unlike eq. (17), this parallel multiplexing of the data results in a better protection against fading thus enhancing the overall diversity order of the system. In other words, if fading results in the loss of some symbols along the direct link, the parity bits that are transmitted over the parallel indirect link (that might not be in fading) might help in the efficient reconstruction of the information symbols. Finally, note that the inequalities in equations (16) and (17) follow from the fact that the block code might correct some error patterns of $t+1$ or more errors.

Finally, integrating the conditional BER given in eq. (16) over the Rayleigh distributions of the components of the vector A results in the following expression of the average BER:

$$P_e \leq \sum_{i=t+1}^N \sum_{t_0=1}^{\min(i,K)} \sum_{\substack{t_1=1 \\ t_0+t_1=i}}^{\min(i,N-K)} \binom{K}{t_0} P_0^{t_0} (1-P_0)^{K-t_0} \binom{N-K}{t_1} P_1^{t_1} (1-P_1)^{N-K-t_1} \quad (17)$$

where P_0 and P_1 correspond to the average error probabilities along the

direct and indirect links. P_0 follows from integrating eq. (14) and takes the value:

$$P_0 = \frac{1}{2} \frac{1}{1 + \frac{K}{N} \lambda_s} \quad (18)$$

while P_1 follows from integrating eq. (7) and takes the value:

$$P_1 = \frac{1}{2} \left[\frac{1}{1 + \frac{1}{2} \frac{N-K}{N} \beta_1 \lambda_s} + \frac{1}{1 + \frac{1}{2} \frac{N-K}{N} \beta_2 \lambda_s} - \frac{1}{1 + \frac{1}{2} \frac{N-K}{N} \beta_1 \lambda_s} \frac{1}{1 + \frac{1}{2} \frac{N-K}{N} \beta_2 \lambda_s} \right] \quad (19)$$

4 SCHEME-2: PARALLEL BEC CHANNEL

4.1 Cooperation Strategy

Unlike the first scheme, the relay now does not forward all the symbols it receives to the destination. This second diversity scheme corresponds to a selective protocol where the relay performs some kind of selection on the symbols that it forwards to the destination. The role of the relay is as follows. If the vector Y_k has one nonzero component, then the relay decides in favor of this slot and forwards the symbol r_k (that will be equal to c_k in this case) to the destination. On the other hand, when Y_k is equal to the all-zero vector, the relay backs off and stops its transmission thus not forwarding the corresponding symbol to the destination. This is the major difference between the two proposed cooperation schemes where for this second scheme; the relay does not make a random choice among the two PPM slots. In the same way, the destination also will not make any

choice in a random manner in the case where both PPM slots have a zero photoelectron count whether along the link S-D or along the link R-D. In this case, when X_k or Z_k is all-zero, the destination will declare an erasure (instead of making a random guess). At a second time, the destination will try to determine the values of the erased symbols by treating them as unknowns when solving the parity-check equations pertaining to the deployed block channel code. The decoding strategy at the destination will be explained in more details in section 4.3. Finally, since the transmitted symbols are taken from the set $\{1,2\}$ while the decoded symbols can be this set or can be equal to an erasure (i.e. no decision is made at the relay or at the destination), then scheme two is analogous to a three-way parallel binary erasure channel (BEC).

4.2 Raw Bit-Error-Rate

Proposition 2: for scheme 2, the probability of erasure along the indirect link S-R-D is given by:

$$p_{e,1} = e^{-k_1} + e^{-k_2} - e^{-(k_1+k_2)} \quad (20)$$

where the constants k_1 and k_2 are defined in eq. (8).

Proof: The probability of erasure can be written as:

$$p_{e,1} = 1 - p_{c,1} \quad (21)$$

where $p_{c,1}$ corresponds to the probability of transmitting a symbol taken from $\{1,2\}$ along the indirect link S-R-D and receiving the same symbol at the destination. Now a correct decision will be made at the destination if and only if a correct decision was also made at the relay (since otherwise the relay is backing off and an erasure will be declared at the destination). In other words, a symbol will be detected

correctly along the link S-R-D if and only if Y_k as well as Z_k contain both nonzero components. Consequently, $p_{c,1}$ can be written as:

$$p_{c,1} = \Pr(Y_{k,c_k} > 0) \Pr(Z_{k,r_k} > 0) \quad (22)$$

where, from eq. (5),

$$\Pr(Y_{k,c_k} > 0) = 1 - \Pr(Y_{k,c_k} = 0) = 1 - e^{-k_1}$$

where the constant k_1 is given in eq. (8).

On the other hand, from eq. (6),

$$\Pr(Z_{k,r_k} > 0) = 1 - \Pr(Z_{k,r_k} = 0) = 1 - e^{-k_2}$$

where the constant k_2 is given in eq. (8).

Replacing these probabilities in eq. (22) results in:

$$p_{c,1} = (1 - e^{-k_1})(1 - e^{-k_2}) \quad (23)$$

Now, from eq. (21):

$$\begin{aligned} p_{e,1} &= 1 - (1 - e^{-k_1})(1 - e^{-k_2}) \\ &= e^{-k_1} + e^{-k_2} - e^{-(k_1+k_2)} \end{aligned} \quad (24)$$

thus proving proposition 2.

Comparing eq. (7) to eq. (20) shows that the probability of making an erroneous hard decision along the link S-R-D and the probability of declaring an erasure along this link differ only by a ratio of $\frac{1}{2}$ which corresponds to the probability of making a wrong random hit among the two PPM time slots.

4.3 Coded Bit-Error-Rate

First, we denote by $p_{e,0}$ the probability of erasure along the direct link S-D:

$$p_{e,0} = \Pr(X_{k,s_k} = 0) = e^{-k_0} \quad (25)$$

The decision at the destination will be based on the N -dimensional vector $S = [\hat{s}_1 \ \dots \ \hat{s}_K \ \hat{c}_1 \ \dots \ \hat{c}_{N-K}]$. Based on the decoding strategy at the relay and the destination, elements of S can be either symbols from $\{1,2\}$ that are detected correctly without any level of uncertainty or erasure symbols that can be treated as unknowns whose values are

to be determined. Now, the decoding procedure at the destination corresponds to determining the values of these unknowns by taking advantage of the symbols that were detected correctly. Since the vector S stands for the received vector corresponding to a certain transmitted codeword, then it must satisfy the $N-K$ parity-check equations that are obtained from:

$$SH^T = 0_{N-K,1} \quad (26)$$

where H stands for the parity-check matrix of the block code while $0_{N-K,1}$ stands for the all-zero vector having $N-K$ rows and one column. Treating eq. (26) as a deterministic system of $N-K$ equations in a certain number of unknowns (corresponding to the erased symbols) shows that it is possible to determine the values of at most $N-K$ erased symbols that are determined from the remaining symbols that are correct with no ambiguity. It is also worth noting that we are interested in solving for the erased values among $\hat{s}_1, \dots, \hat{s}_K$; in this context, the role of the un-erased values among $\hat{c}_1, \dots, \hat{c}_{N-K}$ is to help for solving for the values of the information symbols without being target values to be solved by themselves.

Assume that zero values among $\hat{c}_1, \dots, \hat{c}_{N-K}$ are in erasure. In this case, eq. (26) can correct up to $N-K$ erased values among $\hat{s}_1, \dots, \hat{s}_K$. In general, assume that t_e values among $\hat{c}_1, \dots, \hat{c}_{N-K}$ are in erasure. The probability of this event is given by:

$$P(t_e) = \binom{N-K}{t_e} p_{e,1}^{t_e} (1 - p_{e,1})^{N-K-t_e} \quad (27)$$

where the probability of erasure $p_{e,1}$ along the indirect link is given in eq. (20). Now, when these t_e erasures occur along the indirect link S-R-D, eq. (26)

can correctly determine the values of the remaining $N-K-t_e$ erasures among the symbols $\hat{s}_1, \dots, \hat{s}_K$. In other words, some information symbols will be lost in this case when $N-K-t_e+1$ or more erasures occur along the direct link. Consequently, based on eq. (27), the conditional probability of error when scheme 2 is deployed can be upper-bounded by:

$$P_{e|A} = \sum_{t_e=0}^{N-K} \binom{N-K}{t_e} p_{e,1}^{t_e} (1-p_{e,1})^{N-K-t_e} \sum_{i=N-K-t_e+1}^K \binom{K}{i} p_{e,0}^i (1-p_{e,0})^{K-i} \quad (28)$$

where the probability of erasure $p_{e,0}$ along the direct link is given in eq. (25). Comparing equations (16) and (28) shows that the two cooperation strategies result in different error probabilities at the destination.

Finally, integrating over the Rayleigh distributions of the path gains a_0, a_1 and a_2 results in the following expression of the average coded BER:

$$P_e = \sum_{t_e=0}^{N-K} \binom{N-K}{t_e} P_{e,1}^{t_e} (1-P_{e,1})^{N-K-t_e} \sum_{i=N-K-t_e+1}^K \binom{K}{i} P_{e,0}^i (1-P_{e,0})^{K-i} \quad (29)$$

where $P_{e,0}$ follows from integrating eq. (25) and takes the value:

$$P_{e,0} = \frac{1}{1 + \frac{K}{N} \lambda_s} \quad (30)$$

while $P_{e,1}$ follows from integrating eq. (20) and takes the value:

$$P_{e,1} = \frac{1}{1 + \frac{1}{2} \frac{N-K}{N} \beta_1 \lambda_s} + \frac{1}{1 + \frac{1}{2} \frac{N-K}{N} \beta_2 \lambda_s} - \frac{1}{1 + \frac{1}{2} \frac{N-K}{N} \beta_1 \lambda_s} \frac{1}{1 + \frac{1}{2} \frac{N-K}{N} \beta_2 \lambda_s}$$

Note that both cooperation strategies can be implemented in the absence of channel state information (CSI) at the source, relay and destination. In other words, the proposed schemes are suitable for FSO systems with IM/DD and they do not result in a major complexity in the transceivers' architecture compared to non-cooperative systems. On the other hand, since the cooperation strategies were considered in the absence of background radiation, they can serve as lower bounds on the performance levels that can be achieved in systems that suffer from background radiation. Finally, the analysis that was presented in this paper in the case of Rayleigh fading can be easily extended to other fading models.

5 DIVERSITY ORDERS

In this section, we evaluate the diversity orders that can be achieved by the proposed cooperation strategies for asymptotic values of E_s .

5.1 Scheme-1

Equation (18) shows that P_0 scales asymptotically as λ_s^{-1} for sufficiently large values of λ_s (note that the signal energy E_s and λ_s are two proportional quantities). In the same way, the error probability P_1 given in eq. (19) behaves asymptotically as λ_s^{-1} because the term containing λ_s^{-2} can be neglected compared to λ_s^{-1} for large values of λ_s .

The error performance of scheme 1 is given in eq. (17). For large values of λ_s , $P_0 \ll 1$ and $P_1 \ll 1$ resulting in $1-P_0 \approx 1$ and $1-P_1 \approx 1$. Consequently,

the summation in eq. (17) can be approximated by:

$$P_e \cong \sum_{i=t+1}^N \sum_{t_0=1}^{\min(i,K)} \sum_{\substack{t_1=1 \\ t_0+t_1=i}}^{\min(i,N-K)} \binom{K}{t_0} \binom{N-K}{t_1} P_0^{t_0} P_1^{t_1} \quad (31)$$

Given that $t_0 + t_1 = i$ while the minimum value of i is $t+1$, then eq. (31) scales asymptotically as:

$$P_e \cong \lambda_s^{-\min(t_0+t_1)} = \lambda_s^{-\min_{i=t+1 \dots N}(i)} = \lambda_s^{-(t+1)} \quad (32)$$

showing that the first cooperation strategy is capable of achieving a diversity order of $t+1$. Replacing t by its value from eq. (15) results in:

$$d_1 = \left\lfloor \frac{d_{\min} + 1}{2} \right\rfloor \quad (33)$$

where d_1 stands for the diversity order of scheme 1.

5.2 Scheme-2

As for scheme 1, the probabilities $P_{e,0}$ and $P_{e,1}$ in eq. (29) both scale asymptotically as λ_s^{-1} . Ignoring the probabilities $1-P_{e,0}$ and $1-P_{e,1}$ in this equation results in:

$$P_e \cong \sum_{t_e=0}^{N-K} \binom{N-K}{t_e} P_{e,1}^{t_e} \sum_{i=N-K-t_e+1}^K \binom{K}{i} P_{e,0}^i \quad (34)$$

For $P_{e,1} > P_{e,0}$, the dominant term in the above summation corresponds to the minimum value of t_e (which is $t_e = 0$). In this case, eq. (34) can be approximated by the following expression:

$$P_e \cong \binom{K}{N-K+1} P_{e,0}^{N-K+1} \quad (35)$$

which scales asymptotically as $\lambda_s^{-(N-K+1)}$ for large values of λ_s .

On the other hand, for $P_{e,0} > P_{e,1}$, the dominant term in eq. (34) corresponds to the minimum value of i (which is $i = N-K-(N-K)+1=1$). In this case, t_e takes its

maximum value of $t_e = N-K$ and eq. (34) can be approximated by the following expression:

$$P_e \cong \binom{N-K}{N-K} P_{e,1}^{N-K} \binom{K}{1} P_{e,0}^1 \quad (36)$$

which simplifies to:

$$P_e \cong K P_{e,1}^{N-K} P_{e,0}^1 \quad (37)$$

which scales asymptotically as $\lambda_s^{-(N-K+1)}$ for large values of λ_s .

Since both equations (35) and (37), that correspond to the two possible asymptotic values of P_e , both scale asymptotically as $\lambda_s^{-(N-K+1)}$, then the diversity order that can be achieved by the second cooperation strategy is:

$$d_2 = N - K + 1 \quad (38)$$

where d_2 stands for the diversity order of scheme 2.

Equations (33) and (38) show that the proposed cooperation strategies do not result in the same diversity order. Moreover, d_1 depends on the minimum distance of the channel code implying that the diversity order of scheme-1 depends on the particular structure of the channel code where, as in classical non-cooperative systems, the code must be constructed in a way to maximize d_{\min} . On the other hand, a rather surprising result resides in the fact that d_2 does not depend on the error correction capability of the channel code that is determined by the parameter d_{\min} . In this case, the diversity order of scheme-2 depends only on the number of added parity bits (that is equal to $N-K$ bits per codeword). In this case, it is not necessary for the channel code to have any particular structure and any parity bits added at the end of the information bits will ensure the same performance levels. In particular, the same sequence of parity

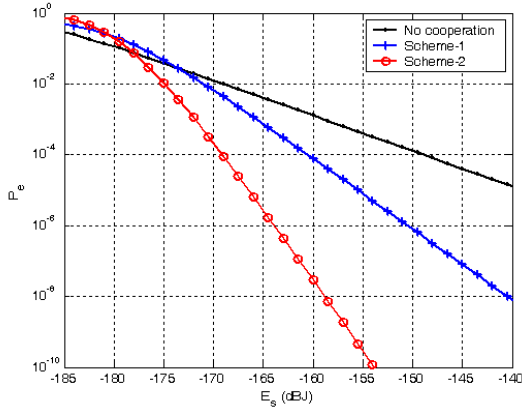


Figure 1. Performance with the (7,4) Hamming code with $\beta_1 = \beta_2 = 1$.

bits $\hat{c}_1, \dots, \hat{c}_{N-K}$ can be added to any information sequence $\hat{s}_1, \dots, \hat{s}_K$. As a special case, for the uncoded case, $N=K$ and $d_{\min} = 1$ resulting in $d_1 = 1$ and $d_2 = 1$ from equations (33) and (38), respectively. In other words, in this case, the proposed schemes are equivalent to non-cooperative systems where the diversity order over the Rayleigh fading channels is equal to 1.

6 NUMERICAL RESULTS

In this section, we present some numerical results that support the analytical results obtained in sections 3, 4 and 5. The path gains a_0, a_1 and a_2 of the three links S-D, S-R and R-D are generated independently from each other. We consider the case of a quasi-static channel that is fixed over 1000 symbol durations while the simulation results are numerically integrated over 10,000 channel realizations. The above assumption of block fading is particularly valid for FSO systems where the turbulence induced fading varies in the order of 1–100 ms [16] while the signal rates under consideration vary from several hundreds to several thousands of Mbps.

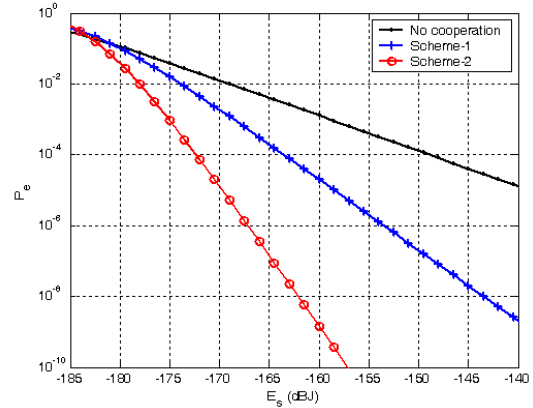


Figure 3. Performance with the (7,4) Hamming code with $\beta_1 = \beta_2 = 4$.

Fig. 2 shows the performance of the proposed cooperation strategies in the case where the (7,4) Hamming code is applied. In this case, 4 information bits are transmitted along the direct link S-D while 3 parity bits are transmitted along the indirect link S-R-D. This code has a minimum distance of $d_{\min}=3$ and is capable of correcting $t = 1$ error from eq. (15). In this figure, we fix $\beta_1 = \beta_2 = 1$ implying that the distances between the source, relay and destination are all the same. This corresponds to an extreme case where there is no energy gain in the system. The obtained results show that the proposed cooperation strategies are capable of achieving very high performance gains especially for large values of E_s . For example, at a BER of 10^{-4} , scheme-1 outperforms non-cooperative systems by about 10 dB while this performance gains increases to about 20 dB with scheme-2. This figure also shows that equations (33) and (38) correctly predict the diversity order of the system. While the diversity order of non-cooperative systems is 1 (the BER drops by a factor of 10 when E_s increases by 10 dB), the diversity order of scheme-1 is equal to 2 (the BER drops by a factor of 10 when E_s increases by 5 dB) while scheme-2 achieves the very

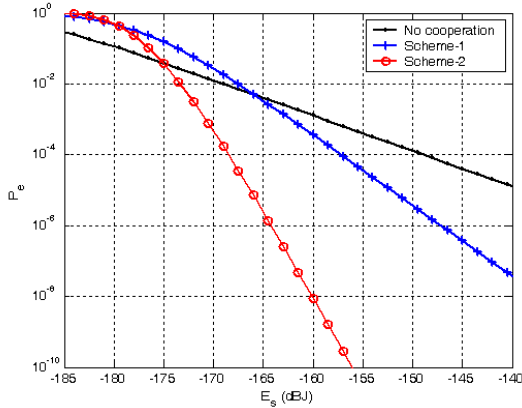


Figure 4. Performance with the (15,11) Hamming code with $\beta_1 = \beta_2 = 1$.

high diversity order of $d_2 = 4$ (the BER drops by a factor of 10 when E_s increases by 2.5 dB).

The simulation setup of Fig. 2 is reproduced in Fig. 3 for $\beta_1 = \beta_2 = 4$. In this case, $d_{SR} = d_{RD} = \frac{1}{2} d_{SD}$ implying that, in this case, the relay is closer to the source and destination. In this case, the performance gains that can be achieved by the proposed cooperation schemes are further enhanced. For example, at a BER of 10^{-4} , the performance gain of scheme-1 increases from 10 dB (for $\beta_1 = \beta_2 = 1$) to about 14.5 dB while scheme-2 results in the very large performance gain of about 23.5 dB. On the other hand, the diversity orders are the same as in Fig.2 since these diversity orders depend on the deployed channel code and not on the gains β_1 and β_2 . Figures 2 and 3 show that cooperation is not useful for all values of E_s . In particular, it is better not to cooperate for small values of E_s since dedicating a part of the small available energy to the indirect link and the non-reliable reconstruction of the parity bits at the relay allow non-cooperative systems to outperform scheme-1 and scheme-2 for this range of values of E_s . However, while for $\beta_1 = \beta_2 = 1$, scheme-1 (resp. scheme-2)

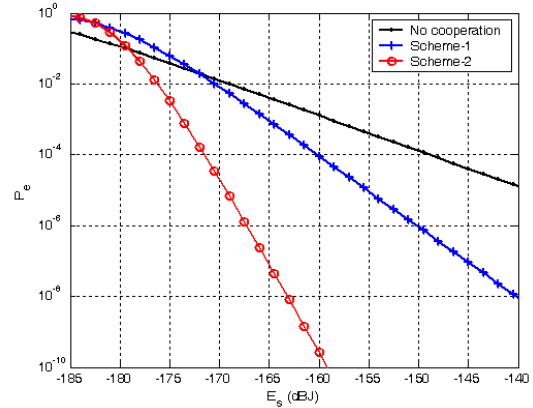


Figure 5. Performance with the (15,11) Hamming code with $\beta_1 = \beta_2 = 4$.

outperforms non-cooperative systems for values of E_s exceeding -173.6 dBJ (resp. -178 dBJ), these values drop to -181 dBJ (resp. -183 dBJ) for $\beta_1 = \beta_2 = 4$. Note that in practical systems, the relay is selected to be close enough to the source and destination implying that the results in Fig. 3 reflect more efficiently the behavior of the cooperation strategies in real life situations.

Figures 4 and 5 show the performance with the (15,11) Hamming code for $\beta_1 = \beta_2 = 1$ and $\beta_1 = \beta_2 = 4$, respectively. This code has a minimum Hamming distance of $d_{min}=3$. The obtained results show that, compared to figures 2 and 3, the diversity order of scheme-1 remains the same since both codes have the same minimum distance while the diversity order of scheme-2 is enhanced from 4 to 5. Note that the decoding complexities of the (7,4) and (15,11) Hamming codes are practically the same when these codes are deployed with scheme-1. On the other hand, when associated with scheme-2, the decoding of the (7,4) Hamming code requires solving a system of 3 equations while the (15,11) Hamming code requires solving a system of 4 equations in up to a maximum number of 4 unknowns.

7 CONCLUSION

In this paper, we investigated joint channel-diversity coding as a powerful and simple distributed fading mitigation technique for non-coherent FSO systems with IM/DD. In particular, we have shown that tackling the three-way cooperative system as a parallel BEC by appropriate encoding/decoding strategies at the relay and destination results in very high performance gains and diversity orders with acceptable system complexity and without any reduction in the data rate. Moreover, this approach does not require applying any particular code structure. On the other hand, tackling the three-way cooperative FSO system as a parallel BSC channel by applying the classical hard-decision decoding technique can be highly suboptimal for such systems.

8 REFERENCES

1. Kedar, D., Arnon, S.: Urban Optical Wireless Communications Networks: the main challenges and possible solutions. *IEEE Communications Magazine*, vol. 42, pp. 2--7 (2003).
2. Willebrand, H., Ghuman, B.S.: *Free Space Optics: Enabling Optical Connectivity in Today Networks*. Sams Publishing (2002).
3. Zhu, X., Kahn, J.M.: Free-Space Optical Communications through Atmospheric Turbulence Channels. *IEEE Transactions on Communications*, vol. 50, pp. 1293--1300 (2002).
4. Zhu, X., Kahn, J.M.: Performance Bounds for Coded Free-Space Optical Communications through Atmospheric Turbulence Channels. *IEEE Transactions on Communications*, vol. 51, pp. 1233--1239 (2003).
5. Riediger, M.L.B., Schober, R., Lample L.: Fast Multiple-Symbol Detection for Free-Space Optical Communications. *IEEE Transactions on Communications*, vol. 57, pp. 1119--1128 (2009).
6. Wilson, S.G., Brandt-Pearce, M., Cao, Q., Baedke, M.: Optical repetition MIMO Transmission with Multipulse PPM. *IEEE journal on Selected Areas in Communications*, vol. 23, pp. 1901--1910 (2005).
7. Khalighi, M.-A., Shwartz, N., Aitamer, N., Bourennane, S.: Fading Reduction by Aperture Averaging and Spatial Diversity in Optical Wireless Systems. *IEEE Journal of Optical Communications and Networking*, vol. 1, pp. 580--593 (2009).
8. Wilson, S.G., Brandt-Pearce, M., Cao, Q., Leveque, J.H.: Free-space Optical MIMO Transmission with Q-ary PPM, *IEEE Transactions on Communications*, vol. 53, pp. 1402--1412 (2005).
9. Simon, M.K., Vilnrotter, V.A.: Alamouti-type Space-Time Coding for Free-Space Optical Communication with Direct Detection. *IEEE Transactions on Wireless Communications*, vol. 4, pp. 35--39 (2005).
10. Garcia-Zambrana, A., Castillo-Vazquez, C., Castillo-Vazquez, B., Hiniesta-Gomez, A.: Selection Transmit Diversity for FSO Links Over Strong Atmospheric Turbulence Channels. *IEEE Photon Technology Letters*, vol. 21, pp. 1017--1019 (2009).
11. Karimi, M., Nasiri-Kenari, M.: Free-Space Optical Communications via Optical Amplify-and-Forward Relaying. *IEEE/OSA journal of Lightwave Technology*, vol. 29, pp. 242--248 (2011).
12. Safari, M., Uysal M.: Relay-Assisted Free-Space Optical Communication. *IEEE Transactions on Wireless Communications*, vol. 7, pp. 5441--5449 (2008).
13. Abou-Rjeily, C., Slim, A.: Cooperative Diversity for Free-Space Optical Communications: Transceiver Design and Performance Analysis. *IEEE Transactions on Communications*, vol. 59, pp. 658--663 (2011).
14. Abou-Rjeily, C.: Cooperative FSO Systems: Performance Analysis and Optimal Power Allocation. *IEEE/OSA journal of Lightwave Technology*, vol. 29, pp. 1058--1065 (2011).
15. Karimi, M., Nasiri-Kenari, M.: BER Analysis of Cooperative Systems in Free-Space Optical Networks. *IEEE/OSA journal of Lightwave Technology*, vol. 27, pp. 5639--5647 (2009).
16. Lee, E., Chan, V.: Part 1: Optical Communication over the Clear Turbulent Atmospheric Channel Using Diversity. *IEEE Journal on Selected Areas in Communications*, vol. 22, pp. 71 896--1906 (2004).